





Outage probability analysis and adaptive combiner for multiuser multipolarized antenna systems

Abdul Hai Muzammil MOHAMMED^{1,2} , Muhammad MOINUDDIN^{1,2} ,
Ubaid Mohsin AL-SAGGAF^{1,2} , Ahmad Kamal HASSAN^{1,3} 

¹Centre of Excellence in Intelligent Engineering Systems, King Abdulaziz University, Jeddah, Saudi Arabia

²Department of Electrical and Computer Engineering, King Abdulaziz University, Jeddah, Saudi Arabia

³Faculty of Electrical Engineering, Ghulam Ishaq Khan Institute of Engineering Sciences and Technology, Topi, Pakistan

Received: 23.11.2017

Accepted/Published Online: 26.08.2018

Final Version: 22.01.2019

Abstract: In this paper, we characterize the performance metrics of a multiuser multipolarized antenna system in a Rayleigh fading channel. We start by formulating a downlink system model that features a multiuser scenario in the presence of additive noise and a multipolarized antenna system; this is followed by evaluation of the outage probability in closed form. This is done by deriving the cumulative distribution function (CDF) of the signal-to-interference-plus-noise ratio using the approach of the ratio of indefinite quadratic forms. We thereby characterize the gradient of this CDF with respect to the combining vectors. Eventually, we obtain the optimum combining vectors by minimizing the outage probability via interior-point optimization technique. Simulation and theoretical results of our analysis are closely matched, which validates our analysis. Our findings suggest that the performance of the triple polarized antenna is better than that of the dual polarized antenna system for low signal-to-noise ratio (SNR) values in terms of outage probability; this situation, however, reverses for high SNR value.

Key words: Multiple-input multiple-output, wireless communications, outage probability, cross-polarization discrimination, signal-to-interference-plus-noise ratio

1. Introduction

Multiple-input multiple-output (MIMO) systems often employ polarization diversity to increase spectral efficiency and link reliability in wireless communication systems. The use of multipolarized antennas at the transmitter and receiver results in compatibility and robustness of devices [1,2]. High-quality multimedia streaming services require higher data rates, such as 8k ultra high definition, whereas virtual reality services also require high data rates. To fulfill these requirements, one can employ a large antenna array MIMO system; however, this will not be a cost-effective solution, besides the difficulty in incorporating a huge antenna array in handheld or compact devices. On the other hand, a multipolarized antenna system has a low correlation even if it is co-located and hence it can be the best solution for realizing compact and robust devices [3]. Incorporation of dual polarized (DP) and triple polarized (TP) antennas with MIMO systems is also a strong candidate for existing and the upcoming fifth generation (5G) wireless communication systems [4,5]. It is to be noted here that the work in [4] makes use of TP antennas to utilize an extra degree of freedom and high data rates.

In a multiuser downlink network, channel propagation between users and the base station (BS) is mostly

*Correspondence: akhassan@theiet.org

modeled by small-scale fading, large-scale fading, and the cross-polarization effect of multipolarized antennas. In order to understand the performance of multipolarized antennas, considerations of cross-polarization discrimination (XPD) and cross-correlation coefficients are important factors. Specifically, the XPD is an essential parameter defined as the ratio of the average power received in a co-polarized channel to the average power received in a cross-polarized channel [6], whereas the cross-correlation coefficient is a measure of the correlation between signals appearing at the antenna array with the same or different polarizations. In related works, the authors in [7] provided a comparison of several multipolarized MIMO models and also presented some useful results in terms of channel capacity. In [8], the authors showed that the use of polarization diversity with a combining method enhances the capacity of wireless communication systems. Oestges et al. in [1] studied the advantages of using DP antenna arrays in a multiple channel environment. In [9], the authors considered channel state information (CSI) at the transmitter and presented a solution for beamforming design with partial CSI feedback in a DP MIMO system. The authors in [10] proposed a precoding scheme in which the XPD, spatial correlations, and CSI quality are utilized for multiuser multipolarized massive MIMO systems, and their extension in [11] presented a precoding scheme that reduces the CSI feedback in a multiuser DP MIMO system. The authors in [12] proposed a spatial division multiple access scheme by utilizing DP antenna arrays at the BS for a massive MIMO system operating in a 3D scenario and the results revealed that the proposed scheme increases the throughput of the system by utilizing DP antennas when compared to single polarized antennas. More recently, the authors in [13] proposed a CSI feedback scheme called layered multipath information-based CSI feedback to achieve high spectrum efficiency for DP systems.

It is noteworthy that there exists only a limited number of works [2,4] in the literature that deal with the comparative analysis of DP and TP antenna systems. Specifically, the authors in [2] investigated the performance of DP and TP antenna systems based on experimental results for channel capacity. However, they used a simulation setup in their investigation to compare the experimental work and did not provide a closed-form expression. Moreover, the work in [4] dealt with the comparison of DP and TP antenna systems based on joint transmit and receive antenna selection and presented several results in terms of outage probability (OP). However, that work did not include a multiuser environment. An indefinite quadratic form-based approach was recently applied to OP characterization in [14,15] without considering multipolarized antennas and receive gain combining techniques. To the best of the authors' knowledge, the performance metrics in terms of the OP without CSI at the transmitter have not been investigated for multiuser multipolarized antenna systems and their special cases such as DP and TP systems.

Our major contributions in the proposed work are in:

- (1) Providing a closed-form solution of OP in a multiuser multipolarized antenna system in a downlink scenario without considering CSI at the transmitter.
- (2) Depicting a comprehensive comparative analysis of DP and TP antenna systems and investigating a suitable signal-to-noise ratio (SNR) range in which the DP antenna system outperforms the TP antenna system and vice versa.
- (3) Utilizing the interior-point optimization technique and deriving a closed-form expression of the gradient of OP with respect to the combining vectors.

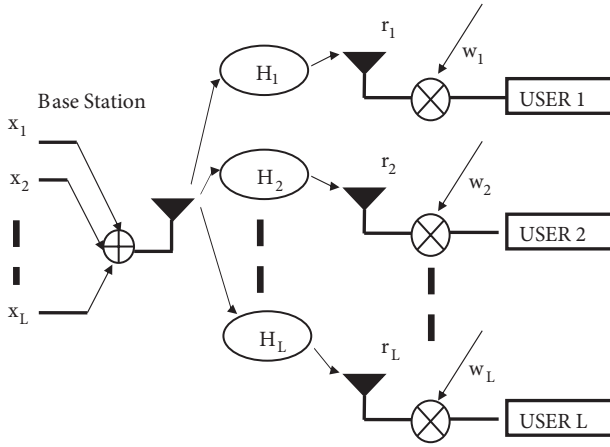
Note that supervised precoding can only be done at the transmitter provided that the CSI is available therein, which is not true in our case. More precisely, in our case, we consider a blind technique that requires only statistical CSI (instead of instantaneous CSI) to design the optimum combiner at the receiver.

After this introduction, in Section 2, we present a system model for the downlink scenario. In Section 3, a review of DP and TP channels is provided. In Section 4, the OP of the multiuser multipolarized antenna system for the downlink scenario is derived. Section 5 provides the adaptive combining design for downlink with DP and TP antennas. In Section 6, simulation results are compared with derived expressions. Finally, Section 7 illustrates our conclusion.

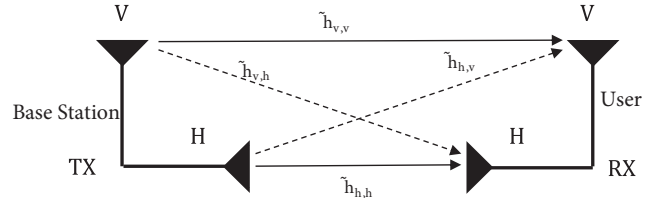
In the notation, all lowercase letters represent scalars, all lowercase letters with bold font represent vectors, and all uppercase boldface letters represent matrices. The notations $()^*$ and $()^H$ represent the conjugate and conjugate transposition, respectively, and $E\{\cdot\}$ denotes expectation and $\text{Tr}(\cdot)$ represents the trace operator.

2. System model

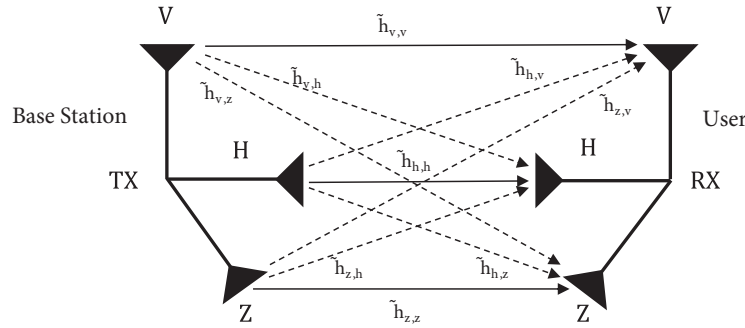
We consider a downlink environment in which a single BS is broadcasting a data stream to L users through a polarized channel \mathbf{H}_i as shown in Figure 1a. The data received by the i th user are given as



(a) Block diagram of downlink multiuser multipolarized communication system



(b) Interlink between DP



(c) Interlink between TP

Figure 1. Downlink multiuser multipolarized communication system.

$$\boldsymbol{\eta}_i = \sum_{l=1}^L \mathbf{H}_i \mathbf{x}_l + \mathbf{n}_i, \quad (1)$$

where $\boldsymbol{\eta}_i = [\eta_1, \eta_2, \dots, \eta_p]^T$ is the received data signal vector of the i th user, and p represents polarization order, such that $p = 2$ for the DP antenna while $p = 3$ for the TP antenna. Furthermore, $\mathbf{x}_l = [x_1, x_2, \dots, x_p]^T$, $\forall l$, is the correlated transmit data signal vector with a distinct correlation factor; \mathbf{n}_i is the zero-mean complex Gaussian noise vector of the i th user satisfying $\mathbf{E}\{\mathbf{n}_i \mathbf{n}_i^H\} = \sigma_i^2 \mathbf{I}_2$; and \mathbf{I}_2 is a $p \times p$ identity matrix. Lastly, \mathbf{H}_i is a $p \times p$ polarization matrix of the i th user whose elements are circular complex Gaussian variables with zero mean, which represents the Rayleigh channel with uniform phase distribution [16]. The variance depends on propagation conditions and the antenna characteristics, which are described later.

Now we combine the received data by using combining vector $\mathbf{w}_i = [w_{i_1}, w_{i_2}, \dots, w_{i_p}]^T$ as follows:

$$z_i = \mathbf{w}_i^H \boldsymbol{\eta}_i = \mathbf{w}_i^H \mathbf{H}_i \mathbf{x}_i + \mathbf{w}_i^H \sum_{l=1, l \neq i}^L \mathbf{H}_i \mathbf{x}_l + \mathbf{w}_i^H \mathbf{n}_i, \quad (2)$$

where the first term in Eq. (2) represents the desired user data, the second term denotes the interference term containing data of other users, and the third term is additive white noise.

The signal-to-interference-plus-noise ratio (SINR) at the input of the receiver for the downlink scenario for the i th user is given by:

$$SINR_i = \frac{|\mathbf{w}_i^H \mathbf{H}_i \mathbf{x}_i|^2}{\left| \mathbf{w}_i^H \mathbf{H}_i \sum_{l=1, l \neq i}^L \mathbf{x}_l \right|^2 + \|\mathbf{w}_i\|^2 \sigma_i^2}. \quad (3)$$

The numerator in Eq. (3) can be rewritten as:

$$|\mathbf{w}_i^H \mathbf{H}_i \mathbf{x}_i|^2 = (\mathbf{w}_i^H \mathbf{H}_i \mathbf{x}_i)(\mathbf{w}_i^H \mathbf{H}_i \mathbf{x}_i)^*.$$

Now we transform the channel matrix \mathbf{H}_i into a p^2 -dimensional vector by using $\mathbf{h}_i = \text{vec}(\mathbf{H}_i)$ such that \mathbf{h}_i is a circular complex Gaussian vector, i.e. $\mathbf{h}_i \sim \mathcal{CN}(0, \mathbf{R}_i)$ with $\mathbf{R}_i = \mathbf{E}\{\mathbf{h}_i \mathbf{h}_i^H\}$. This transformation allows us to reformulate the numerator as

$$\otimes |\mathbf{w}_i^H \mathbf{H}_i \mathbf{x}_i|^2 = \mathbf{h}_i \{ \mathbf{w}_i \mathbf{w}_i^H \mathbf{x}_i \mathbf{x}_i^H \} \mathbf{h}_i^H.$$

At this stage, we apply the whitening transformation for \mathbf{h}_i as $\tilde{\mathbf{h}}_i = \left(\mathbf{R}_i^{-\frac{1}{2}} \right)^H \mathbf{h}_i$ such that $\tilde{\mathbf{h}}_i$ is a circular white complex Gaussian vector. Thus, the numerator can be written as:

$$|\mathbf{w}_i^H \mathbf{H}_i \mathbf{x}_i|^2 = \tilde{\mathbf{h}}_i^H \mathbf{R}_i^{\frac{1}{2}} \{ \mathbf{w}_i \mathbf{w}_i^H \otimes \mathbf{x}_i \mathbf{x}_i^H \} \mathbf{R}_i^{\frac{H}{2}} \tilde{\mathbf{h}}_i = \left\| \tilde{\mathbf{h}}_i \right\|_{\mathbf{R}_i^{\frac{1}{2}} \{ \mathbf{w}_i \mathbf{w}_i^H \otimes \mathbf{x}_i \mathbf{x}_i^H \} \mathbf{R}_i^{\frac{H}{2}}}^2.$$

Using the same methodology, we can reformulate the denominator as follows:

$$\left| \mathbf{w}_i^H \mathbf{H}_i \sum_{l=1, l \neq i}^L \mathbf{x}_l \right|^2 + \|\mathbf{w}_i\|^2 \sigma_i^2 = \left\| \tilde{\mathbf{h}}_i \right\|_{\mathbf{R}_i^{\frac{1}{2}} \left\{ \mathbf{w}_i \mathbf{w}_i^H \otimes \sum_{l=1, l \neq i}^L \mathbf{x}_l \mathbf{x}_l^H \right\} \mathbf{R}_i^{\frac{H}{2}} + \|\mathbf{w}_i\|^2 \sigma_i^2}^2.$$

As a result, the SINR in Eq. (3) can be simplified as:

$$SINR_i = \frac{\left\| \tilde{\mathbf{h}}_i \right\|_{\mathbf{R}_i^{\frac{1}{2}}}^2 \left\{ \mathbf{w}_i \mathbf{w}_i^H \otimes \mathbf{x}_i \mathbf{x}_i^H \right\}_{\mathbf{R}_i^{\frac{H}{2}}}}{\left\| \tilde{\mathbf{h}}_i \right\|_{\mathbf{R}_i^{\frac{1}{2}}}^2 \left\{ \mathbf{w}_i \mathbf{w}_i^H \otimes \sum_{l=1, l \neq i}^L \mathbf{x}_l \mathbf{x}_l^H \right\}_{\mathbf{R}_i^{\frac{H}{2}}} + \left\| \mathbf{w}_i \right\|^2 \sigma_i^2} \quad (4)$$

The aim here is to derive the OP using the above SINR expression and then to use it in designing adaptive combining weights \mathbf{w}_i . Before proceeding to these tasks, we first present the channel model for DP and TP antennas.

3. Overview of dual and triple polarized channel models

In this section, we provide a brief overview of the dual and triple polarized channel models and also define several parameters that are later used in this work. In this paper, we assume that the data signals are transmitted and received through the same polarization scheme. Interlinks between the sets of DP and TP antenna employed at the transmitter and receiver are shown in Figure 1b and Figure 1c.

3.1. Dual polarized channel model

For the DP antenna system, the channel matrix \mathbf{H}_i has elements that are complex Gaussian random variables with zero mean as given in [17] and reproduced herein as:

$$\mathbf{H}_i = \begin{bmatrix} \tilde{\mathbf{h}}_{v,v} & \tilde{\mathbf{h}}_{v,h} \\ \tilde{\mathbf{h}}_{h,v} & \tilde{\mathbf{h}}_{h,h} \end{bmatrix}.$$

The channel matrix is represented in terms of horizontal (h) and vertical (v) polarizations, such that elements $\tilde{\mathbf{h}}_{h,v}$ and $\tilde{\mathbf{h}}_{v,h}$ correspond to the cross-polarized components (horizontal to vertical and vertical to horizontal polarization of waves) and elements $\tilde{\mathbf{h}}_{h,h}$ and $\tilde{\mathbf{h}}_{v,v}$ are co-polarized components (horizontal to horizontal and vertical to vertical polarization of waves). Herein, we use the model provided by Bolcskei et al. in [16] and also take useful insights from Habib et al. [4] and Coldrey [5]. We express XPD as $XPD = \frac{1-\alpha}{\alpha}$, which is defined as the ratio of the average power received in a co-polarized channel to the average power received in a cross-polarized channel, whereas α is the ability of the antenna to separate orthogonal polarized waves and describes the joint effect of antenna characteristics and channel. The coefficient α has the range of $0 < \alpha \leq 1$. Smaller values of α give perfect discrimination between vertical and horizontal polarized components and vice versa. Furthermore, the experimental data from [18,19] explain that the elements of the matrix are correlated; thus, for the DP system, the correlation coefficients are [16]:

$$t = \frac{\mathbf{E} \left\{ \tilde{\mathbf{h}}_{h,h} \tilde{\mathbf{h}}_{v,h}^* \right\}}{\sqrt{\alpha}} = \frac{\mathbf{E} \left\{ \tilde{\mathbf{h}}_{h,v} \tilde{\mathbf{h}}_{v,v}^* \right\}}{\sqrt{\alpha}}, \quad (5)$$

$$r = \frac{\mathbf{E} \left\{ \tilde{\mathbf{h}}_{h,h} \tilde{\mathbf{h}}_{h,v}^* \right\}}{\sqrt{\alpha}} = \frac{\mathbf{E} \left\{ \tilde{\mathbf{h}}_{v,h} \tilde{\mathbf{h}}_{v,v}^* \right\}}{\sqrt{\alpha}}, \quad (6)$$

where t is the transmit correlation coefficient and r is the receive correlation coefficient.

It is noteworthy that the experimental results [18,19] reveal that the correlation between off-diagonal elements and diagonal elements of the channel matrix is very small, i.e. $\mathbf{E} \left\{ \tilde{\mathbf{h}}_{v,v} \tilde{\mathbf{h}}_{h,h}^* \right\} = \mathbf{E} \left\{ \tilde{\mathbf{h}}_{v,h} \tilde{\mathbf{h}}_{h,v}^* \right\} = 0$. Eventually, by using these correlation values, the covariance matrix $\mathbf{R}_i = \mathbf{E} \left\{ \tilde{\mathbf{h}}_i \tilde{\mathbf{h}}_i^H \right\}$ of DP system can be expressed as:

$$\mathbf{R}_i = \begin{bmatrix} 1 - \alpha & \sqrt{\alpha}t & \sqrt{\alpha}r & 0 \\ \sqrt{\alpha}t & \alpha & 0 & \sqrt{\alpha}r^* \\ \sqrt{\alpha}r & 0 & \alpha & \sqrt{\alpha}t^* \\ 0 & \sqrt{\alpha}r^* & \sqrt{\alpha}t^* & 1 - \alpha \end{bmatrix}. \quad (7)$$

3.2. Triple polarized channel model

It is well known in the research community that in order to have an additional degree of freedom, a TP system can be used. This is done by introducing a polarized antenna in the z-direction at both the transmitter and receiver and it is orthogonal to both the DP antennas in x- and y-directions. The TP system channel matrix \mathbf{H}_i can be written as [4]:

$$\mathbf{H}_i = \begin{bmatrix} \tilde{\mathbf{h}}_{v,v} & \tilde{\mathbf{h}}_{v,h} & \tilde{\mathbf{h}}_{v,z} \\ \tilde{\mathbf{h}}_{h,v} & \tilde{\mathbf{h}}_{h,h} & \tilde{\mathbf{h}}_{h,z} \\ \tilde{\mathbf{h}}_{z,v} & \tilde{\mathbf{h}}_{z,h} & \tilde{\mathbf{h}}_{z,z} \end{bmatrix},$$

where the components of the channel matrix $\tilde{\mathbf{h}}_{v,v}$, $\tilde{\mathbf{h}}_{h,h}$, and $\tilde{\mathbf{h}}_{z,z}$ are the co-polarized components and the components $\tilde{\mathbf{h}}_{v,h}$, $\tilde{\mathbf{h}}_{v,z}$, $\tilde{\mathbf{h}}_{h,v}$, $\tilde{\mathbf{h}}_{h,z}$, $\tilde{\mathbf{h}}_{z,h}$, and $\tilde{\mathbf{h}}_{z,v}$ are the cross-polarized components. Furthermore, cross-correlation coefficients for TP antennas are given by [20]:

$$t = \frac{\mathbf{E} \left\{ \tilde{\mathbf{h}}_{h,h} \tilde{\mathbf{h}}_{v,h}^* \right\}}{\sqrt{\alpha}} = \frac{\mathbf{E} \left\{ \tilde{\mathbf{h}}_{h,v} \tilde{\mathbf{h}}_{v,v}^* \right\}}{\sqrt{\alpha}} = \frac{\mathbf{E} \left\{ \tilde{\mathbf{h}}_{h,h} \tilde{\mathbf{h}}_{h,z}^* \right\}}{\sqrt{\alpha}} = \frac{\mathbf{E} \left\{ \tilde{\mathbf{h}}_{h,z} \tilde{\mathbf{h}}_{z,z}^* \right\}}{\sqrt{\alpha}}, \quad (8)$$

$$r = \frac{\mathbf{E} \left\{ \tilde{\mathbf{h}}_{h,h} \tilde{\mathbf{h}}_{h,v}^* \right\}}{\sqrt{\alpha}} = \frac{\mathbf{E} \left\{ \tilde{\mathbf{h}}_{v,h} \tilde{\mathbf{h}}_{v,v}^* \right\}}{\sqrt{\alpha}} = \frac{\mathbf{E} \left\{ \tilde{\mathbf{h}}_{h,h} \tilde{\mathbf{h}}_{z,h}^* \right\}}{\sqrt{\alpha}} = \frac{\mathbf{E} \left\{ \tilde{\mathbf{h}}_{z,h} \tilde{\mathbf{h}}_{z,z}^* \right\}}{\sqrt{\alpha}}. \quad (9)$$

The model provided by Habib et al. [8] for a TP system has the following considerations:

$$\mathbf{E} \left\{ \left| \tilde{\mathbf{h}}_{h,h} \right|^2 \right\} = \mathbf{E} \left\{ \left| \tilde{\mathbf{h}}_{v,v} \right|^2 \right\} = \mathbf{E} \left\{ \left| \tilde{\mathbf{h}}_{z,z} \right|^2 \right\} = 1 - (\alpha_1 + \alpha_2),$$

$$\mathbf{E} \left\{ \left| \tilde{\mathbf{h}}_{v,h} \right|^2 \right\} = \mathbf{E} \left\{ \left| \tilde{\mathbf{h}}_{z,v} \right|^2 \right\} = \mathbf{E} \left\{ \left| \tilde{\mathbf{h}}_{h,z} \right|^2 \right\} = \alpha_1,$$

$$\mathbf{E} \left\{ \left| \tilde{\mathbf{h}}_{h,v} \right|^2 \right\} = \mathbf{E} \left\{ \left| \tilde{\mathbf{h}}_{v,z} \right|^2 \right\} = \mathbf{E} \left\{ \left| \tilde{\mathbf{h}}_{z,h} \right|^2 \right\} = \alpha_2.$$

The XPD for the TP channel can be represented as $XPD = \frac{1 - (\alpha_1 + \alpha_2)}{(\alpha_1 + \alpha_2)}$, where the $\alpha_1 + \alpha_2$ range is $< (\alpha_1 + \alpha_2) \leq 1$. The covariance matrix \mathbf{R}_i for TP systems can be written as $\mathbf{R}_i = \mathbf{E} \left\{ \tilde{\mathbf{h}}_i \tilde{\mathbf{h}}_i^H \right\}$, where \mathbf{R}_i is

a 9×9 matrix, which can be represented as:

$$\mathbf{R}_i = \begin{bmatrix} 1 - \alpha & \sqrt{\alpha t} & \sqrt{\alpha t} & \sqrt{\alpha r} & \sqrt{\alpha r} & 0 & \sqrt{\alpha r} & 0 & 0 \\ \sqrt{\alpha t}^* & \alpha & \sqrt{\alpha t}^* & 0 & \sqrt{\alpha r} & 0 & 0 & \sqrt{\alpha r} & 0 \\ \sqrt{\alpha t}^* & \sqrt{\alpha t}^* & \alpha & 0 & \sqrt{\alpha r} & \sqrt{\alpha r} & 0 & 0 & \sqrt{\alpha r} \\ \sqrt{\alpha r}^* & 0 & 0 & \alpha & \sqrt{\alpha t} & \sqrt{\alpha t} & \sqrt{\alpha r} & 0 & 0 \\ 0 & \sqrt{\alpha r}^* & 0 & \sqrt{\alpha t}^* & 1 - \alpha & \sqrt{\alpha t} & 0 & \sqrt{\alpha r} & 0 \\ 0 & 0 & \sqrt{\alpha r}^* & \sqrt{\alpha r}^* & \sqrt{\alpha r}^* & \alpha & 0 & 0 & \sqrt{\alpha r} \\ \sqrt{\alpha r}^* & 0 & 0 & \sqrt{\alpha r}^* & 0 & 0 & \alpha & \sqrt{\alpha t} & \sqrt{\alpha t} \\ 0 & \sqrt{\alpha r}^* & 0 & 0 & 0 & \sqrt{\alpha r}^* & \sqrt{\alpha t}^* & \alpha & \sqrt{\alpha t} \\ 0 & 0 & \sqrt{\alpha r}^* & 0 & 0 & \sqrt{\alpha r}^* & \sqrt{\alpha t}^* & \sqrt{\alpha t}^* & 1 - \alpha \end{bmatrix}.$$

4. Outage probability of multiuser multipolarized antenna system

In this section, we provide the OP in a closed-form expression for the downlink scenario with multipolarized antennas. Using the SINR given in Eq. (4), the cumulative distribution function (CDF) representing the OP for the i th user based on a given threshold γ denoted as $F(\gamma_i)$ is [14]:

$$F(\gamma_i) = \Pr(\text{SINR}_i < \gamma). \quad (10)$$

Substituting Eq. (4) in Eq. (10) yields

$$\begin{aligned} F(\gamma_i) &= \Pr\left(\|\mathbf{w}_i\|^2 \sigma_i^2 \gamma + \tilde{\mathbf{h}}_i \mathbf{D} \tilde{\mathbf{h}}_i^H < \gamma\right) \\ &= \int_{-\infty}^{\infty} p(\tilde{\mathbf{h}}) u\left(\|\mathbf{w}_i\|^2 \sigma_i^2 \gamma + \tilde{\mathbf{h}}_i \mathbf{D} \tilde{\mathbf{h}}_i^H\right) d\tilde{\mathbf{h}}_i, \end{aligned} \quad (11)$$

where $u(\cdot)$ is the unit step function and matrix \mathbf{D} is defined as

$$\mathbf{D} = \left\{ \mathbf{R}_i^{\frac{1}{2}} \left\{ \mathbf{w}_i \mathbf{w}_i^H \otimes \mathbf{x}_i \mathbf{x}_i^H \right\} \mathbf{R}_i^{\frac{H}{2}} \right\} - \gamma \left\{ \mathbf{R}_i^{\frac{1}{2}} \left\{ \mathbf{w}_i \mathbf{w}_i^H \otimes \sum_{l=1, l \neq i}^L \mathbf{x}_l \mathbf{x}_l^H \right\} \mathbf{R}_i^{\frac{H}{2}} \right\}. \quad (12)$$

We now express our first major result in terms of a closed-form solution for the CDF of OP in a downlink multiuser multipolarized antennas system as

$$F(\gamma_i) = 1 - \sum_{d=1}^T \frac{\lambda_d^T}{|\lambda_d| \prod_{k=1, k \neq d}^T (\lambda_d - \lambda_k)} e^{-\left(\frac{\|\mathbf{w}_i\|^2 \sigma_i^2 \gamma}{\lambda_d}\right)} u\left(\frac{\|\mathbf{w}_i\|^2 \sigma_i^2 \gamma}{\lambda_d}\right), \quad (13)$$

where λ_d represent the d th eigenvalue of matrix \mathbf{D} and T is a variable indicating the total number of eigenvalues of matrix \mathbf{D} .

Proof The proof of Eq. (13) is given in Appendix A. \square

Note that the expression remains the same for both dual and triple polarized antennas. However, matrix \mathbf{D} will take distinct forms for distinct polarized antennas.

5. Adaptive combining design of multiuser multipolarized antenna system

In this section, we outline an optimal solution for the minimization of OP with respect to \mathbf{w}_i expressed in terms of an unconstrained optimization problem as:

$$\min_{\mathbf{w}_i} F(\gamma_i), \forall_i \quad (14)$$

The above optimization problem can be solved in multiple ways. The authors in [21] depicted a useful comparison of well-known optimization techniques, which included the interior-point method and sequential quadratic programming approach. We, however, use the former herein, i.e. the interior-point method, due to its faster convergence in the proposed work. The usefulness of the interior-point method has been applied in various engineering design problems [22,23]. It is noteworthy that mathematical software such as MATLAB, R, and Mathematica give the designer an option to provide the gradient or Hessian of the objective function. In what follows, we provide the gradient of OP given in Eq. (13) in a closed form with respect to the elements of combining vector \mathbf{w}_i as follows:

$$\begin{aligned} \frac{\partial F(\gamma_i)}{\partial w_{i_j}} = & \sum_{d=1}^T \left\{ \left(\left[\alpha_{l,1} w_{ij}^* \sigma_i^2 \gamma + (\alpha_{l,2} \|\mathbf{w}_i\|^2 \sigma_i^2 \gamma + \alpha_{l,3}) \left(\frac{\Sigma_{dd}^-}{|\Sigma^{-1}|} \right) \right] \times \left(e^{-\left(\frac{\|\mathbf{w}_i\|^2 \sigma_i^2 \gamma}{\lambda_d} \right)} u \left(\frac{\|\mathbf{w}_i\|^2 \sigma_i^2 \gamma}{\lambda_d} \right) \right) \right) \right. \\ & \left. + \sum_{g=1, g \neq d}^T \beta_{l,1} \left(e^{-\left(\frac{\|\mathbf{w}_i\|^2 \sigma_i^2 \gamma}{\lambda_g} \right)} u \left(\frac{\|\mathbf{w}_i\|^2 \sigma_i^2 \gamma}{\lambda_g} \right) \right) \right\}, \end{aligned} \quad (15)$$

where w_{i_j} represent the j th element of vector \mathbf{w}_i , and Σ_{dd}^- represent the d th diagonal values of matrix $\bar{\Sigma}$, whose definition follows:

$$\begin{aligned} \bar{\Sigma} &= \mathbf{U}_d^{-1} \Sigma \mathbf{U}_d^{-H}; \quad \Sigma = P\gamma - \mathbf{Q}, \\ \otimes \mathbf{P} &= \mathbf{R}_i^{\frac{1}{2}} \left\{ \frac{\partial \{\mathbf{w}_i \mathbf{w}_i^H\}}{\partial w_{i_j}} \mathbf{x}_i \mathbf{x}_i^H \right\} \mathbf{R}_i^{\frac{H}{2}}, \\ \otimes \mathbf{Q} &= \mathbf{R}_i^{\frac{1}{2}} \left\{ \frac{\partial \{\mathbf{w}_i \mathbf{w}_i^H\}}{\partial w_{i_j}} \sum_{l=1, l \neq i}^L \mathbf{x}_l \mathbf{x}_l^H \right\} \mathbf{R}_i^{\frac{H}{2}}, \end{aligned}$$

while $\alpha_{l,1}$, $\alpha_{l,2}$, $\alpha_{l,3}$, and $\beta_{l,1}$ are the partial fraction expansion coefficients used in Eq. (15) and defined herein as

$$\begin{aligned} \alpha_{l,1} &= \frac{\lambda_d^{T-1}}{|\lambda_d| \prod_{g=1, g \neq d}^T (\lambda_d - \lambda_g)}, \\ \alpha_{l,2} &= \frac{\lambda_d^{T-3}}{\prod_{g=1, g \neq d}^T (\lambda_g) \prod_{g=1, g \neq d}^T \left(\frac{\lambda_d}{\lambda_g} - 1 \right)}, \end{aligned}$$

$$\alpha_{l,3} = \frac{\lambda_d^{T-2}}{\prod_{g=1, g \neq d}^T (\lambda_g) |\lambda_d| \sum_{g=1, g \neq d}^T \left(\frac{\lambda_d}{\lambda_g} - 1 \right) \prod_{g=1, g \neq d}^T \left(\frac{\lambda_d}{\lambda_g} - 1 \right)},$$

$$\beta_{l,1} = \frac{1}{\lambda_d} \prod_{g=1, g \neq d}^T (\lambda_g) |\lambda_d| \sum_{g=1, g \neq d}^T \left(\frac{1}{\lambda_d} - \frac{1}{\lambda_g} \right) \prod_{j=1, j \neq g, d}^T \left(\frac{1}{\lambda_g} - \frac{1}{\lambda_j} \right).$$

Proof The proof of Eq. (15) is given in Appendix B. \square

In our case, the objective function defined in Eq. (14) gives a nonconvex optimization problem. It can produce local as well as global optimum solutions.

6. Simulation results

In this section, we validate the closed-form expression of the multipolarized downlink antenna system given in Eq. (13) by means of an extensive Monte Carlo simulation setup. We consider a single cell scenario in which the BS is equipped with a single $p \times p$ polarized antenna that communicates to L users' equipment, which are also equipped with a single $p \times p$ polarized antenna. Throughout the simulation and analysis, we took an equal gain combining vector (EGC) for comparison of DP and TP antenna systems, in which we consider $w = [0.5, 0.5]$ for DP systems and $w = [0.33, 0.33, 0.33]$ for TP systems. Here, we do not consider instantaneous CSI at the transmitter side and hence we are unable to use maximum ratio combining (MRC). The data matrix $\mathbf{x}_l \mathbf{x}_l^H$, $\forall l$, follows the exponential model with entries $\eta_{s,t} = \eta_i^{|s-t|}$ and with correlation factor η_i with range of $0 < \eta_i < 1$. Our goal in this section is to:

- (1) Show the effect of number of users on OP in both DP and TP antenna systems.
- (2) Observe the effect of XPD coefficient and noise variance on OP.
- (3) Investigate the extent of improvement in system performance by incorporating the interior-point optimization scheme.

In Figure 2, we compare the simulation results with the analytical results for the downlink scenario for different users with DP and TP antennas by using noise variance of $\sigma_i^2 = 0.01$, whereas other parameters are $t = 0.4$, $r = 0.3$, $\alpha = 0.5$ for DP antennas and $\alpha_1 + \alpha_2 = 0.5$ for TP antennas. It is observed that the OP increases by increasing the number of users for both DP and TP antennas. This is due to the fact that an increase in the multipath number leads to an increase in intersymbol interference, which eventually results in the degradation of system performance.

In Figure 3a, we show the effect of XPD coefficient $\alpha_1 + \alpha_2$ on OP for TP antennas for different transmit correlation with $r = 0$, noise variance $\sigma_i^2 = 0.5$, and $L = 4$. It is observed that OP is better at $\alpha_1 + \alpha_2 = 0.9$ when compared to $\alpha_1 + \alpha_2 = 0.15$ for different values of transmit correlation. This is because the low XPD denotes significant leakage between the polarizations and the systems loses most of the energy due to polarization mismatch, whereas at high XPD the system achieves better performance. In Figure 3b, we compare the performance of DP and TP antennas with respect to different noise variances. It is noted that at high variance the TP antenna system outperforms the DP antenna system and this situation reverses for a low

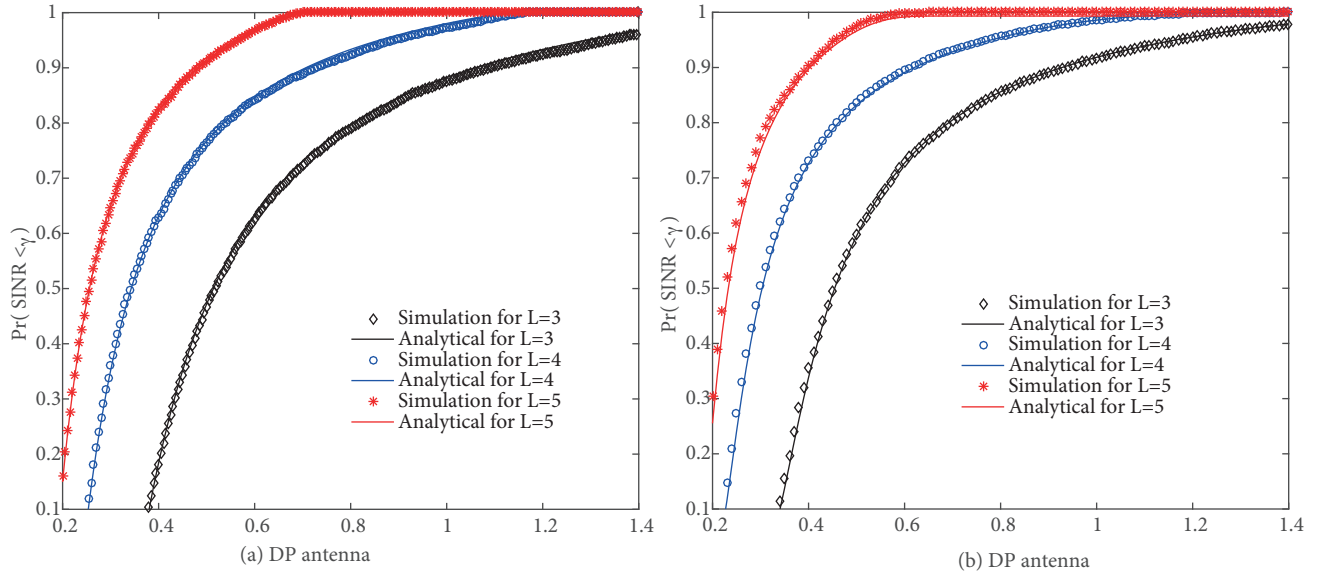


Figure 2. Simulation and analytical results of outage probability for DP and TP antennas for different values of users (L).

variance value. Now, based on the outcome of analytical and simulation results, a roadmap for future frontiers in the field can be made. In Figure 4, we test the interior-point optimization scheme given in Section 4 on the OP metric on both DP and TP antenna systems. It is seen that optimization results of TP antenna systems are better enhanced as compared to the DP antenna system for the parameters set to $r = 0.3$, $\sigma_i^2 = 0.5$, $t = 0.4$, $\alpha = 0.5$, and $\alpha_1 + \alpha_2 = 0.5$.

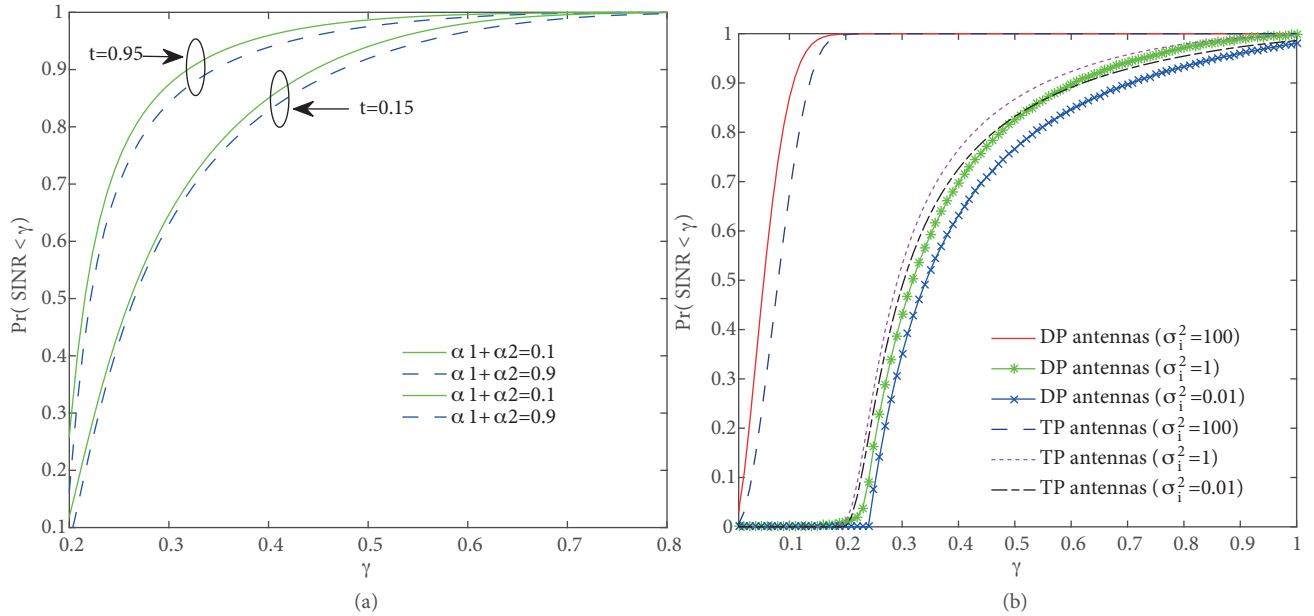


Figure 3. Effect of (a) $\alpha_1 + \alpha_2$ on outage probability for TP antennas for different transmit correlation with $r = 0$ and $\sigma_i^2 = 0.5$, and (b) variance on outage probability of downlink for DP and TP antennas for $t = 0.4$, $r = 0.3$, $\alpha = 0.5$, and $\alpha_1 + \alpha_2 = 0.5$.

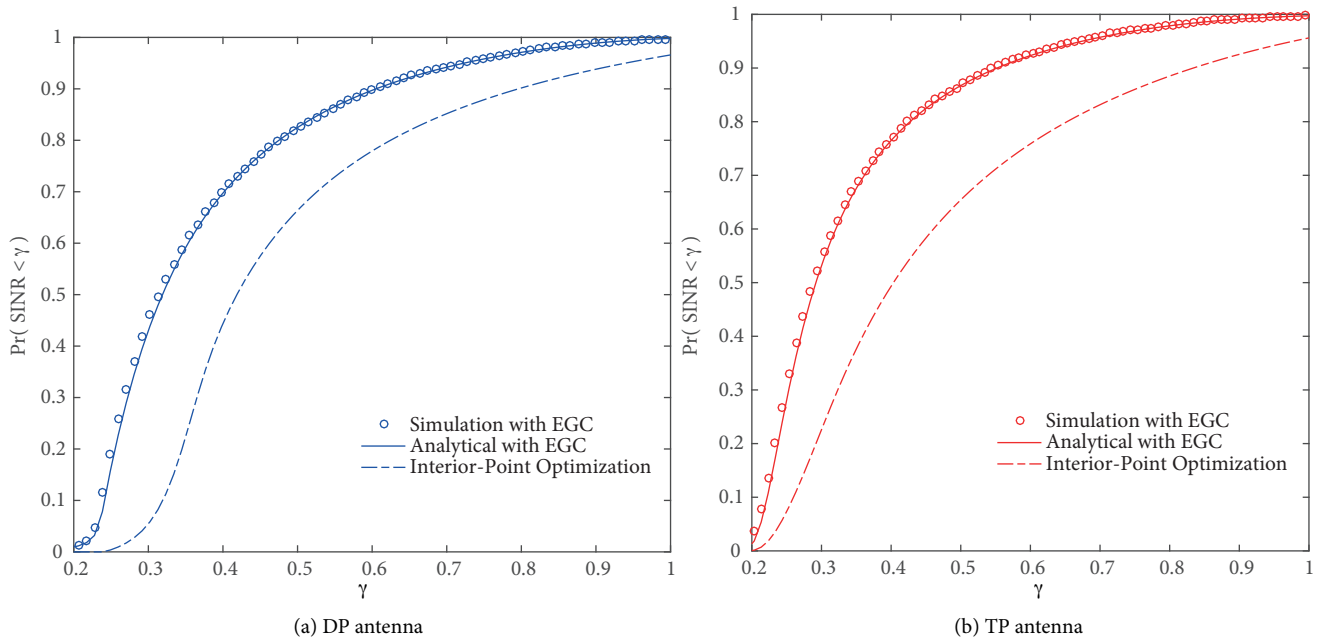


Figure 4. outage probability of downlink for DP and TP antennas with and without optimization for $r = 0.3$, $\sigma_i^2 = 0.5$, $t = 0.4$, $\alpha = 0.5$, and $\alpha_1 + \alpha_2 = 0.5$.

Lastly, in Figure 5a, the performance of DP and TP antenna systems is investigated in terms of OP versus SNR for a threshold value of $\gamma = 0.3$. It is observed that at this threshold, the DP antenna outperforms the TP antenna for most of the SNR range, while the TP polarized antenna performs better only for very low SNR values. This may be due to the fact that higher polarization order antennas can suffer from larger interference, which is more dominant at low SNR values. In Figure 5b, we show the performance of DP and TP antenna

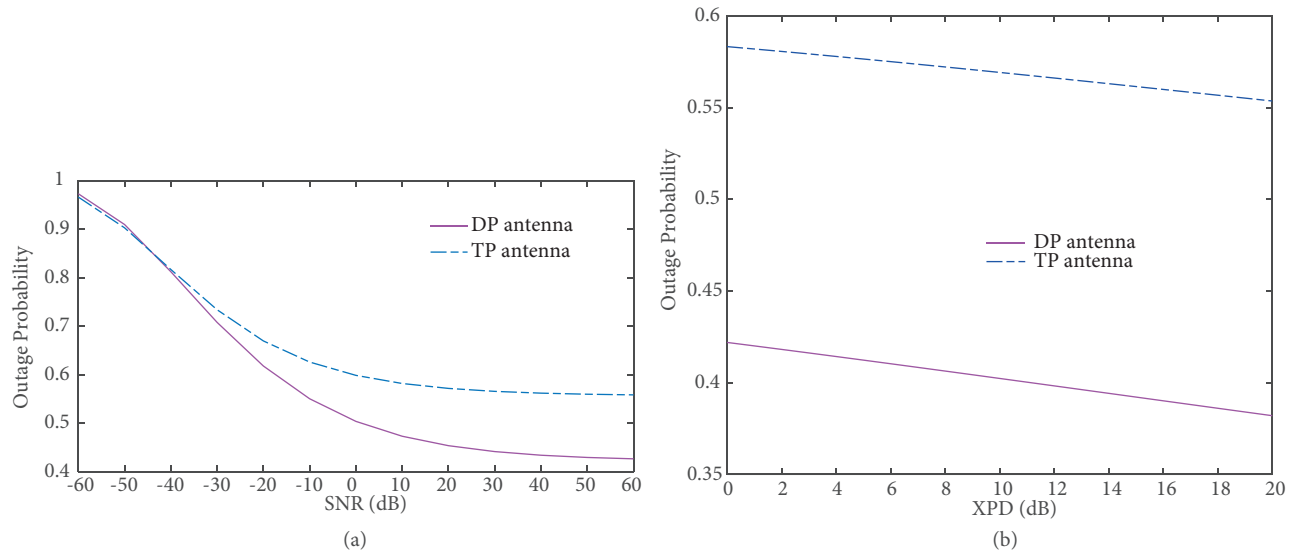


Figure 5. Effect of (a) SNR on outage probability for DP and TP antennas at $\gamma = 0.3$ with transmit correlation $t = 0.4$ with $r = 0.3$ and $\sigma_i^2 = 0.5$, and (b) XPD on outage probability of downlink for DP and TP antennas at $\gamma = 0.3$ with $t = 0.7$, $r = 0.5$, and $\sigma_i^2 = 0.5$.

systems in terms of OP versus XPD for a threshold value of $\gamma = 0.3$ and at SNR equal to 13 dB. Since higher XPD means less cross-polarization interference, this improves the system performance. Therefore, both DP and TP performance improves by increasing the XPD.

7. Conclusion

In this work, we developed an adaptive combining technique for multiuser multipolarized antenna systems by minimizing the probability of outage. This was possible due to the closed-form characterization of outage probability. For the general scenario of the multiuser multipolarized antenna system, we provided a useful comparison of DP and TP antenna systems at different noise variances and investigated the cases in which the TP system outperforms the DP system and vice versa. Our investigation further helped to identify the SNR range in which DP or TP antennas can be more useful. This work provided a very useful foundation for multipolarized systems, which can be extended to multiuser multipolarized MIMO systems.

Acknowledgment

This project was funded by the Centre of Excellence in Intelligent Engineering Systems (CEIES), King Abdulaziz University, under Grant No. CEIES-16-12- 03. The authors therefore acknowledge the technical and financial support of CEIES.

References

- [1] Oestges C, Clerckx B, Guillaud M, Debbah M. Dual-polarized wireless communications: from propagation models to system performance evaluation. *IEEE T Wirel Commun* 2008; 7: 4019-4031.
- [2] Chiu CY, Yan JB, Murch RD. Compact three-port orthogonally polarized MIMO antennas. *IEEE Antenn Wirel Pr* 2007; 6: 619-622.
- [3] Habib A, Krasniqi B, Rupp M. Convex optimization for receive antenna selection in multi-polarized MIMO transmissions. In: *IEEE 19th International Conference on Systems, Signals and Image Processing*; 11 April 2012; Vienna, Austria. New York, NY, USA: IEEE. pp. 269-275.
- [4] Habib A. Multiple polarized MIMO with antenna selection. In: *IEEE 2011 18th Symposium on Communications and Vehicular Technology in the Benelux*; 22 November 2011; Ghent, Belgium. New York, NY, USA: IEEE. pp. 1-8.
- [5] Coldrey M. Modeling and capacity of polarized MIMO channels. In: *IEEE 2008 Spring Vehicular Technology Conference*; 11 May 2008; Singapore. New York, NY, USA: IEEE. pp. 440-444.
- [6] Dao MT, Nguyen VA, Im YT, Park SO, Yoon G. 3D polarized channel modeling and performance comparison of MIMO antenna configurations with different polarizations. *IEEE T Antenn Propag* 2011; 59: 2672-2682.
- [7] He Y, Cheng X, Stuber GL. On polarization channel modeling. *IEEE Wirel Commun* 2016; 23: 80-86.
- [8] Jeon K, Hui B, Chang K, Park H, Park Y. SISO polarized flat fading channel modeling for dual-polarized antenna systems. In: *IEEE 2012 International Conference on Information Networking*; 1 February 2012; Bali, Indonesia. New York, NY, USA: IEEE. pp. 368-373.
- [9] Kim T, Clerckx B, Love DJ, Kim SJ. Limited feedback beamforming systems for dual-polarized MIMO channels. *IEEE T Wirel Commun* 2010; 9: 3425-3439.
- [10] Park J, Clerckx B. Multi-polarized multi-user Massive MIMO: Precoder design and performance analysis. In: *IEEE 2014 Proceedings of the 22nd European Signal Processing Conference*; 1 September 2014; Lisbon, Portugal. New York, NY, USA: IEEE. pp. 326-330.

- [11] Park J, Clerckx B. Multi-user linear precoding for multi-polarized massive MIMO system under imperfect CSIT. *IEEE T Wirel Commun* 2015; 14: 2532-2547.
- [12] Cheng F, Jiang P, Jin S, Huang Q. Dual-polarized spatial division multiple access transmission for 3D multiuser massive MIMO. In: *IEEE 2015 International Conference on Wireless Communications & Signal Processing*; 15 October 2015; Nanjing, China. New York, NY, USA: IEEE. pp. 1-5.
- [13] Zheng F, Chen Y, Zhan Q, Zhang J. An efficient CSI feedback scheme for dual-polarized MIMO systems using layered multi-paths Information. *China Commun* 2017; 14:91-104.
- [14] Al-Naffouri TY, Moinuddin M, Ajeeb N, Hassibi B, Moustakas AL. On the distribution of indefinite quadratic forms in Gaussian random variables. *IEEE T Commun* 2016; 64:153-165.
- [15] Hassan AK, Moinuddin M, Al-Saggaf UM, Al-Naffouri TY. Performance analysis of beamforming in MU-MIMO systems for Rayleigh fading channels. *IEEE Access* 2017; 5: 3709-3720.
- [16] Bolcskei H, Nabar RU, Erceg V, Gesbert D, Paulraj AJ. Performance of spatial multiplexing in the presence of polarization diversity. In: *IEEE 2001 International Conference on Acoustics, Speech, and Signal Processing*; 7–11 May 2001; Utah, USA. New York, NY, USA: IEEE. pp. 2437-2440.
- [17] Nabar RU, Bolcskei H, Erceg V, Gesbert D, Paulraj AJ. Performance of multi-antenna signaling techniques in the presence of polarization diversity. *IEEE T Signal Proces* 2002; 50: 2553-2562.
- [18] Nabar RU, Erceg V, Bölcskei H, Paulraj AJ. Performance of multi-antenna signaling strategies using dual-polarized antennas: measurement results and analysis. *Wireless Pers Commun* 2002; 23: 31-44.
- [19] Baum DS, Gore D, Nabar R, Panchanathan S, Hari KV, Erceg V, Paulraj AJ. Measurement and characterization of broadband MIMO fixed wireless channels at 2.5 GHz. In: *IEEE 2000 International Conference on Personal Wireless Communications*, 17–20 December 2000; Hyderabad, India. New York, NY, USA: IEEE. pp. 203-206.
- [20] Habib A. Antenna selection for compact multiple antenna communication systems. PhD, Vienna University of Technology, Vienna, Austria, 2012.
- [21] Betts JT, Gablonsky JM. A Comparison of Interior Point and SQP Methods on Optimal Control Problems. Phantom Works Mathematics and Computing Technology, Technical Report, March 2002.
- [22] Fuhrmann DR, San Antonio G. Transmit beamforming for MIMO radar systems using signal cross-correlation. *IEEE T Aero Elec Sys* 2008; 44: 171-186.
- [23] Palomar DP, Cioffi JM, Lagunas MA. Joint Tx-Rx beamforming design for multicarrier MIMO channels: a unified framework for convex optimization. *IEEE T Signal Proces* 2003; 51: 2381-2401.
- [24] Ahmed R, Al-Saggaf UM, Moinuddin M, Hassan AK. Mitigation of self-interference and multi-user interference in downlink multi-user MIMO system. *IET Commun* 2017; 11: 2605-2612.
- [25] Gradshteyn IS, Ryzhik IM. *Table of Integrals, Series, and Products*. 7th ed. San Diego, CA, USA: Academic Press, 2014.

A. Proof of outage probability of downlink for multipolarized antennas.

In order to evaluate the multidimensional integral in Eq. (11), we employ the approach given in [9,24]. Since $\tilde{\mathbf{h}}_i$ is a circular white Gaussian vector, the pdf of $\tilde{\mathbf{h}}_i$ is given as

$$p(\tilde{\mathbf{h}}_i) = \frac{1}{\pi^T} e^{-\|\tilde{\mathbf{h}}_i\|^2}.$$

Now we replace the unit step function in Eq. (11) by its Fourier representation [9]:

$$u(x) = \frac{1}{2\pi} \int_{-\infty}^{\infty} \frac{e^{x(j\omega+\beta)}}{(j\omega+\beta)} d\omega; \beta > 0$$

Therefore, the CDF of Eq. (11) can be expressed as

$$\begin{aligned} F(\gamma_i) &= \frac{1}{2\pi^{T+1}} \int_{-\infty}^{\infty} \frac{e^{\|\mathbf{w}_i\|^2 \sigma_i^2 \gamma (j\omega+\beta)}}{(j\omega+\beta)} \\ &\quad \times \left[\int_{-\infty}^{\infty} e^{-\|\tilde{\mathbf{h}}_i\|^2} e^{-\mathbf{R}_i^{\frac{1}{2}} \left\{ \mathbf{w}_i \mathbf{w}_i^H \otimes \sum_{l=1, l \neq i}^L \mathbf{x}_l \mathbf{x}_l^H \right\} \mathbf{R}_i^{\frac{H}{2}} \gamma (j\omega+\beta) + \mathbf{R}_i^{\frac{1}{2}} \left\{ \mathbf{w}_i \mathbf{w}_i^H \otimes \mathbf{x}_i \mathbf{x}_i^H \right\} \mathbf{R}_i^{\frac{H}{2}} (j\omega+\beta)} d\tilde{\mathbf{h}}_i \right] d\omega \\ &= \frac{1}{2\pi} \int_{-\infty}^{\infty} \frac{e^{\|\mathbf{w}_i\|^2 \sigma_i^2 \gamma (j\omega+\beta)}}{(j\omega+\beta) \prod_{d=1}^T 1 + \lambda_d (j\omega+\beta)} d\omega, \end{aligned} \quad (\text{A.1})$$

where the second equality is based on the solution of the complex Gaussian integral, whereas λ_d represent the d th eigenvalue of matrix \mathbf{D} .

Next, by the partial fraction expansion of Eq. (A.1), we have

$$F(\gamma_i) = \frac{1}{2\pi} \int_{-\infty}^{\infty} \frac{e^{\|\mathbf{w}_i\|^2 \sigma_i^2 \gamma (j\omega+\beta)}}{(j\omega+\beta)} d\omega - \frac{1}{2\pi} \int_{-\infty}^{\infty} e^{\|\mathbf{w}_i\|^2 \sigma_i^2 \gamma (j\omega+\beta)} \sum_{d=1}^T \frac{1}{1 + \lambda_d (j\omega+\beta)} \frac{\lambda_d^{T+1}}{\prod_{k=1, k \neq d}^T (\lambda_d - \lambda_k)} d\omega. \quad (\text{A.2})$$

By applying the residue theory defined in [25] to Eq. (A.2) and considering a case of distinct eigenvalue without repetition, we achieve Eq. (13).

B. Proof of Eq. (15).

From Eq. (11), the derivative for the j th element of vector \mathbf{w}_i formulates as

$$\frac{\partial F(\gamma_i)}{\partial w_{ij}} = \int_{-\infty}^{\infty} p(\tilde{\mathbf{h}}_i) \left\{ w_{ij}^* \sigma_i^2 \gamma + \hat{h}_i \boldsymbol{\Sigma} \hat{h}_i^H \right\} \delta \left(\|\mathbf{w}_i\|^2 \sigma_i^2 \gamma + \tilde{\mathbf{h}}_i \mathbf{D} \tilde{\mathbf{h}}_i^H \right) d\tilde{\mathbf{h}}_i = I_1 + I_2, \quad (\text{B.1})$$

where I_1 formulates as

$$I_1 = w_{ij}^* \sigma_i^2 \gamma \sum_{d=1}^T \left\{ \alpha_{l,1} \times e^{-\left(\frac{\|\mathbf{w}_i\|^2 \sigma_i^2 \gamma}{\lambda_d} \right)} u \left(\frac{\|\mathbf{w}_i\|^2 \sigma_i^2 \gamma}{\lambda_d} \right) \right\}. \quad (\text{B.2})$$

Next, I_2 is expressed as follows”

$$\begin{aligned} I_2 &= \int_{-\infty}^{\infty} p(\tilde{\mathbf{h}}_i) \tilde{\mathbf{h}}_i \Sigma \tilde{\mathbf{h}}_i^H \delta \left(\|\mathbf{w}_i\|^2 \sigma_i^2 \gamma + \tilde{\mathbf{h}}_i \Sigma \tilde{\mathbf{h}}_i^H \right) d\tilde{\mathbf{h}}_i \\ &= \frac{1}{2\pi} \int_{-\infty}^{\infty} e^{\|\mathbf{w}_i\|^2 \sigma_i^2 \gamma (j\omega + \beta)} \times I_{2A} d\omega, \end{aligned} \quad (\text{B.3})$$

where $\Sigma = \mathbf{P}\gamma - \mathbf{Q}$. Furthermore, Σ can be decomposed as $\Sigma = \Sigma^{\frac{H}{2}} \Sigma^{\frac{1}{2}}$ and the inner integral in the second equality, i.e. I_{2A} , formulates as

$$\begin{aligned} I_{2A} &= \frac{1}{\pi^M} \int_{-\infty}^{\infty} \left\| \tilde{\mathbf{h}}_i \right\|_{\Sigma}^2 e^{-\|\tilde{\mathbf{h}}_i\|_{I+\mathbf{D}(j\omega+\beta)}^2} d\tilde{\mathbf{h}}_i \\ &= \frac{1}{\pi^M} \int_{-\infty}^{\infty} \left\| \hat{\mathbf{h}}_i \right\|^2 e^{-\hat{\mathbf{h}}_i^H \Sigma^{\frac{H}{2}} \Sigma^{-\frac{H}{2}} \{I+(\mathbf{D})(j\omega+\beta)\} \Sigma^{-\frac{1}{2}} \Sigma^{\frac{1}{2}} \hat{\mathbf{h}}_i} d\tilde{\mathbf{h}}_i \\ &= \frac{1}{\pi^M} \int_{-\infty}^{\infty} \left\| \hat{\mathbf{h}}_i \right\|^2 e^{-\hat{\mathbf{h}}_i^H \Sigma^{-\frac{H}{2}} \{I+(\mathbf{D})(j\omega+\beta)\} \Sigma^{-\frac{1}{2}} \hat{\mathbf{h}}_i} d\hat{\mathbf{h}}_i \\ &= \frac{1}{\pi^M} \int_{-\infty}^{\infty} \left\| \hat{\mathbf{h}}_i \right\|^2 e^{-\|\hat{\mathbf{h}}_i\|_{\Sigma^{-\frac{H}{2}} \{I+(\mathbf{D})(j\omega+\beta)\} \Sigma^{\frac{1}{2}}}^2} d\hat{\mathbf{h}}_i, \end{aligned} \quad (\text{B.4})$$

where $\hat{\mathbf{h}}_i \sim CN(0, \Sigma^{\frac{1}{2}})$. Next, we define a matrix \mathbf{X} as $\mathbf{X} = \Sigma^{-\frac{H}{2}} \{I + (\mathbf{D})(j\omega + \beta)\} \Sigma^{-\frac{1}{2}}$, and therefore I_{2A} can therefore be expressed as

$$I_{2A} = \frac{\text{Tr}(\mathbf{X}^{-1})}{\det(\mathbf{X})}. \quad (\text{B.5})$$

Solving the denominator term of Eq. (B.5) yields

$$\det(\mathbf{X}) = \left| \Sigma^{-\frac{H}{2}} \{I + (\mathbf{D})(j\omega + \beta)\} \Sigma^{-\frac{1}{2}} \right| = |\Sigma|^{-1} |I + \wedge(j\omega + \beta)|,$$

where, in the second equality, we have used the determinant property of the Hermitian matrix.

Now solving the numerator term of Eq. (B.5) follows:

$$\begin{aligned} \text{Tr}(\mathbf{X}^{-1}) &= \text{Tr} \left(\Sigma^{-\frac{H}{2}} \{I + (\mathbf{D})(j\omega + \beta)\} \Sigma^{-\frac{1}{2}} \right)^{-1} \\ &= \text{Tr} \left(\Sigma \{I + (\mathbf{D})(j\omega + \beta)\}^{-1} \right) \\ &= \text{Tr} \left(\left(\bar{\Sigma} \{I + (\mathbf{D})(j\omega + \beta)\}^{-1} \right) \right) \\ &= \sum_{d=1}^T \frac{\bar{\Sigma}_{dd}}{1 + \lambda_d(j\omega + \beta)}, \end{aligned} \quad (\text{B.6})$$

where $\bar{\Sigma} = \mathbf{U}_d^{-1} \Sigma \mathbf{U}_d^{-H}$, in the second equality we have used the property $\text{Tr}(\mathbf{AB})^{-1} = \mathbf{B}^{-1} \mathbf{A}^{-1}$, and in the third equality we have used $\text{Tr}(\mathbf{ABC}) = \text{Tr}(\mathbf{BCA})$.

Thus, by substituting $Tr(\mathbf{X}^{-1})$ and $det(\mathbf{X})$ in Eq. (B.5), we obtain the following expression:

$$\begin{aligned}
 I_{2A} &= \sum_{d=1}^T \frac{\bar{\Sigma}_{dd}}{1 + \lambda_d(j\omega + \beta)} \times \frac{|\Sigma|}{\prod_{d=1}^T (1 + \lambda_d(j\omega + \beta))} \\
 &= \sum_{d=1}^T \left(\frac{\bar{\Sigma}_{dd}}{|\Sigma^{-1}|} \right) \left\{ \frac{\alpha_{l,2}}{(1 + \lambda_d(j\omega + \beta))^2} + \frac{\alpha_{l,3}}{(1 + \lambda_d(j\omega + \beta))} + \sum_{g=1, g \neq d}^T \frac{\beta_{l,1}}{(1 + \lambda_g(j\omega + \beta))} \right\}. \quad (\text{B.7})
 \end{aligned}$$

Eventually, substituting Eq. (B.7) in Eq. (B.3) yields

$$\begin{aligned}
 I_2 &= \sum_{d=1}^T \left\{ \left(\frac{\bar{\Sigma}_{dd}}{|\Sigma^{-1}|} \right) \left(\left[(\alpha_{l,2} \|\mathbf{w}_i\|^2 \sigma_i^2 \gamma + \alpha_{l,3}) \right] \times \left(e^{-\left(\frac{\|\mathbf{w}_i\|^2 \sigma_i^2 \gamma}{\lambda_d} \right)} u \left(\frac{\|\mathbf{w}_i\|^2 \sigma_i^2 \gamma}{\lambda_d} \right) \right) \right. \right. \\
 &\quad \left. \left. + \sum_{g=1, g \neq d}^T \beta_{l,1} \left(e^{-\left(\frac{\|\mathbf{w}_i\|^2 \sigma_i^2 \gamma}{\lambda_g} \right)} u \left(\frac{\|\mathbf{w}_i\|^2 \sigma_i^2 \gamma}{\lambda_g} \right) \right) \right\}. \quad (\text{B.8})
 \end{aligned}$$

Thus, with the aid of Eqs. (B.1), (B.2), and (B.8), we achieve the latest expression given in Eq. (15).